Water Air Soil Pollut (2021) 232:124
https://doi.org/10.1007/s11270-021-05047-w

Magnetic Biomonitoring Using Native Lichens: Spatial Distribution of Traffic-Derived Particles

Rocío Q. Gómez · Marcos A.E. Chaparro · Mauro A.E. Chaparro · Ana G. Castañeda-Miranda · Débora C. Marié · José D. Gargiulo · Harald N. Böhnel

Received: 5 October 2020 / Accepted: 10 February 2021

Abstract Air pollution has become a subject of extensive study of several disciplines and it is identified as one of the most damaging factors for the ecosystem and human health. In urban areas, particle emission can be found in suspension and therefore a portion of them is inhalable for humans, or deposited on streets and several surfaces, including lichen's thallus. We studied particulate matter (PM) (by traffic emission) accumulated in native lichens *Parmotrema pilosum* in order to carry out a magnetic biomonitoring over 2016 and 2017. For this purpose, the environmental magnetism method was complemented with inductively coupled plasma optical emission spectrometry, scanning electron microscopy, and geostatistical methods. The accumulated iron oxides on lichen's thallus include potential toxic elements, such as Ba, Cr, Ni, and V. Fe-rich particles related to vehicle emissions correspond to (ultra)fine magnetite of inhalable sizes ($PM_{2.5}$). Our results indicate a relation between concentration of magnetic particles and areas with high traffic, as well as the influence of rainfall on magnetic PM records. Magnetic biomonitoring is validated as a low-cost and complementary methodology to determine levels of air magnetic PM pollution in cities.

Keywords Biomonitor · Geostatistics · Magnetic proxy · Particle pollution · Traffic emission

1 Introduction

Vehicular traffic is known as one of the major, if not the largest, sources of air pollution source in urban environments. Airborne traffic-related particulate matter (PM) is emitted mainly by exhaust pipes (gasoline- and diesel-powered vehicles), brake lining system, tire debris, and re-suspension of road dust (Rogge et al. 1993; Almeida et al. 2005; Lawrence et al. 2013). Particle emission includes inhalable particulate matter and potentially toxic elements (PTE) that spread due to atmospheric circulation. Such PM emission is not only a damaging factor for the ecosystem but also harmful to human health. In particular, the small size of particles is a key point because $PM_{2.5}$ and $PM_{1.0}$ can reach the deepest parts of the lungs and the smallest ones the alveoli. Therefore, they increase the risk of respiratory illness, asthma (Brauer et al. 2002), and cardiovascular diseases (Mills et al. 2009), as well as the increase in mortality (Nel 2005). PM exposure may also create oxidative stress and inflammation in the brain directly after the entry of

R. Q. Gómez · M. A. Chaparro (✉) · A. G. Castañeda-Miranda · D. C. Marié · J. D. Gargiulo
Centro de Investigaciones en Física e Ingeniería del Centro de la Provincia de Buenos Aires (CIFICEN, CONICET-UNCPBA), Pinto 399, 7000 Tandil, Argentina
e-mail: chapator@exa.unicen.edu.ar

M. A. Chaparro
Centro Marplatense de Investigaciones Matemáticas (CEMIM-UNMDP-CONICET), Diagonal J. B. Alberdi, 2695 Mar del Plata, Argentina

H. N. Böhnel
Centro de Geociencias, UNAM, Boulevard Juriquilla No. 3001, 76230 Juriquilla, QRO, Mexico

Published online: 16 March 2021

particles into the human brain (Maher et al. 2016), or indirectly via stimulation of peripheral/systemic inflammation (Block and Calderón-Garcidueñas 2009; Genc et al. 2012).

Lichens are considered one of the most useful biological indicators of environmental changes. Although they are sensitive to different pollutants, some of them (e.g., *Hypogymnia physodes*, *Xanthoria parietina*, *Parmotrema pilosum*, etc.) are pollution-tolerant species that can be used as biological collectors or biomonitors of air pollutants such as particulate matter, metals, and other pollutants (NO_2, SO_2, HF, etc.) (Rhoades 1999; Kováčik et al. 2011; Sett and Kundu 2016). Thus, lichen utilization for biomonitoring of air pollution in urban areas has increased (Carreras and Pignata 2002; Zschau et al. 2003; Calvelo and Liberatore 2004; Bermudez et al. 2009; Boamponsem and de Freitas 2017).

Although one of the first studies of magnetic particles trapped by biological collectors were reported in the 1990s (Flanders 1994; Huhn et al. 1995), detailed magnetic biomonitoring studies have gained importance in environmental magnetism in the last decades. This methodology has been used as a useful tool to study particle pollution in urban and industrial areas through magnetic parameters in a wide range of biological materials such as tree leaves, pine needles, trunk woods, mosses, *Tillandsia* spp., lichens, etc. (Maher and Thompson 1999; Evans and Heller 2003; Castañeda-Miranda et al. 2016).

Among these biomonitors, epiphytic species such as lichens are passive collectors that incorporate airborne PM into their thalli over long periods (up to several years). Magnetic biomonitoring studies have taken advantage of this fact and that magnetic properties of accumulated particles are suitable proxies for pollution, which allow identifying adversely impacted zones within study areas. From the 2010s (Jordanova et al. 2010; Salo et al. 2012; Chaparro et al. 2013; Kodnik et al. 2017; Marié et al. 2018), three methodologies have been defined for lichens in magnetic biomonitoring, that is, (1) the lichen native species collection; (2) the lichen transplant technique; and (3) "in situ magnetic biomonitoring" or biomonitoring using in situ measurements of magnetic susceptibility, as detailed in Marié et al. (2018, 2020). These methodologies allow us to assess particle pollution; however, differences between them arise from (a) the choice of exposure time for PM collection (weeks, months, years), (b) the possibility of determining the initial conditions of exposure, (c) the preservation species, and (d) the use of available native species to record air pollution over the lichen's life.

Given the adverse consequences of traffic emission in urban areas, the present study focus on assessing the air PM pollution by magnetic biomonitoring using native lichens; in this study case, the selected species is *Parmotrema pilosum*. It allows us to contribute with new information for comparison and refine the methodology, which is low cost and easily replicable in a densely populated city, as well as in other cities with available lichen species. The main objectives for this study are (i) to characterize magnetic particles collected by lichen samples; (ii) to determine their potential threat through the particle size distribution and element composition; (iii) to obtain prediction maps for the spatial distribution of magnetic PM and analyze changes over 1 year; and (iv) to compare it with available results reported around the world.

2 Sampling and Methods

2.1 Sampling

The study area is located in Mar del Plata City (38° 0.1368' S; 57° 33.4524' W), one of the largest cities (619,000 inhabitants, National 2010 Census) in SE of Buenos Aires Province in Argentina (Fig. 1). A high number of vehicles per person are reported in this city. According to the I Annual Report of Mar del Plata (2015), the number of vehicles (560,000) including cars, motorcycles, and heavy transport can be increased significantly, approximately 25% of the total, during holiday seasons. Most of buildings within the study area comprise textile stores, warehouses, public buildings, and private ones; on the other hand, the industrial area is far away. Therefore, vehicle emission is the main air pollution source in this area. Based on this characteristic, the study area includes avenues with a large flux of vehicles and residential zones with less vehicular traffic that allows to compare different (impacted) zones.

Two sampling campaigns of well-distributed native lichen (*P. pilosum*) were carried out in April 2016 (Campaign 2016, 25 April 2016–05 May 2016) and in March 2017 (Campaign 2017, 06 March 2017–29 March 2017) in areas of 7.0–8.5 km^2. Selection of sampling sites was based on geostatistical techniques, designing an initial study area of about 2.65 km by 2.65 km, with a sampling grid of two to three blocks

(~ 0.2–0.3 km). After each sampling campaign was realized, a total of 105 lichen samples were collected. Lichens living on trees were selected and sampled at 1.5 m height above ground in order to avoid the influence of soil particles. Each lichen was carefully collected using plastic scrapers and tools to avoid contamination and then they were stored in paper bags to prevent the formation of possible fungi (as proposed by Marié et al. 2016). Samples were labeled as ml (Campaign 2016) and mlv (Campaign 2017).

2.2 Methods

Samples were stored and sub-sampled at the Environmental Magnetism laboratory of CIFICEN-UNCPBA where most of magnetic measurements were done. Lichens were dried, ground, weighted (0.3–1.2 g) and prepared for different analyses. The material was packed in plastic containers of 2.3 cm^3 for magnetic susceptibility and remanent magnetization measurements and in nonmagnetic quartz glass sample holder (5.5 mm in diameter and 16 mm length) for thermomagnetic measurements. A minimum quantity was used for microscopy analysis, and pulverized material was used for chemical analyses.

Details of environmental magnetism measurements can be found in Chaparro et al. (2013). Magnetic concentration-dependent parameters such as specific magnetic susceptibility (χ), anhysteretic remanent magnetization (ARM), anhysteretic susceptibility (χ_{ARM}), and saturation of isothermal remanent magnetization (SIRM) were measured. Among these parameters, χ is a well-recognized magnetic proxy of pollution. It has the fundamental advantages of high sensitivity and speed, ease of sample preparation, relatively low cost laboratory instruments for data acquisition, and measurements that are nondestructive (Chaparro et al. 2014). Magnetic susceptibility measurements were made using the magnetic susceptibility meter MS2 (Bartington Instruments Ltd.) linked to the MS2B dual-frequency sensor (0.47 and 4.7 kHz). These measurements were done on the higher sensitivity range (0.1×10^{-5} SI), and they were corrected for drift through five measurement cycles (two air readings and three sample readings). The accuracy of the magnetic susceptibility measurement is 1%. The ARM was imparted using a device attached to a shielded demagnetizer (Molspin Ltd.), superimposing a DC bias field of 90 μT (71.6 A/m) to a peak alternating field (AF) of 100 mT, and an AF decay rate of 17 μT per cycle. The remanent magnetization was measured with a spinner fluxgate magnetometer (Minispin, Molspin Ltd.), which has a noise level $< 2.5 \times 10^{-5}$ A/m and a sensitivity of 10^{-4} A/m. χ_{ARM} was calculated using linear regression for ARM acquired at two DC bias fields of 50 and 90 μT (39.8 and 71.6 A/m). The IRM studies were performed using a pulse magnetizer model IM-10-30 (ASC Scientific). Each sample was magnetized by exposing it to stepwise incrementing DC fields, from 1.7 to 2470 mT. The remanent magnetization after each step was measured using the abovementioned Minispin magnetometer. The measured magnetic parameters and ratios described as magnetic mineralogy-dependent parameters (remanent coercivity H_{cr} or B_{cr}, and S-ratio = - IRM_{-300mT}/SIRM)) and magnetic grain size-dependent parameters (percentage frequency-dependent susceptibility χ_{FD}%, SIRM/χ, and anhysteretic ratios χ_{ARM}/χ and ARM/SIRM) were calculated. Thermomagnetic measurements (M – T heating/cooling curves) were made using a laboratory-made horizontal magnetic translation balance (Escalante and Böhnel 2011). The magnetic field (0.5 T) was produced by a special shape of pole pieces of an electromagnet; the temperature was measured with a thermocouple (Type E) located in a furnace close to the sample and controlled using a PID temperature controller (Watlow®). The magnetic force was compensated and recorded (PicoLog® recorder) with a position sensor that generates an output voltage when the balance is deflected. Measurements were performed in air, and each sample was heated to a temperature of about 700 °C and then cooled to room temperature (RT) with a controlled heating/cooling rate of 30 °C/ min.

On the other hand, description of element analysis and scanning electron microscopy methods can be found in Mejía-Echeverry et al. (2018). The elements V, Cr, Co, Ni, Cu, Zn, Mo, Ba, Pb, and Fe were determined in 30 lichen samples by inductively coupled plasma optical emission spectrometry (ICP-OES) at the Laboratory of Chemical Analysis (LANAQUI, CERZOS-CONICET-UNS, Argentina). The determinations for each sample correspond to average values of two independent replicates, all within a percentage standard deviation < 2.5%. Lichen's thalli were examined by scanning electron microscopy and X-ray energy-dispersive spectroscopy (SEM-EDS) at the Centro de Geociencias (UNAM, Mexico). These studies allow us to carry out a morphological characterization of particles

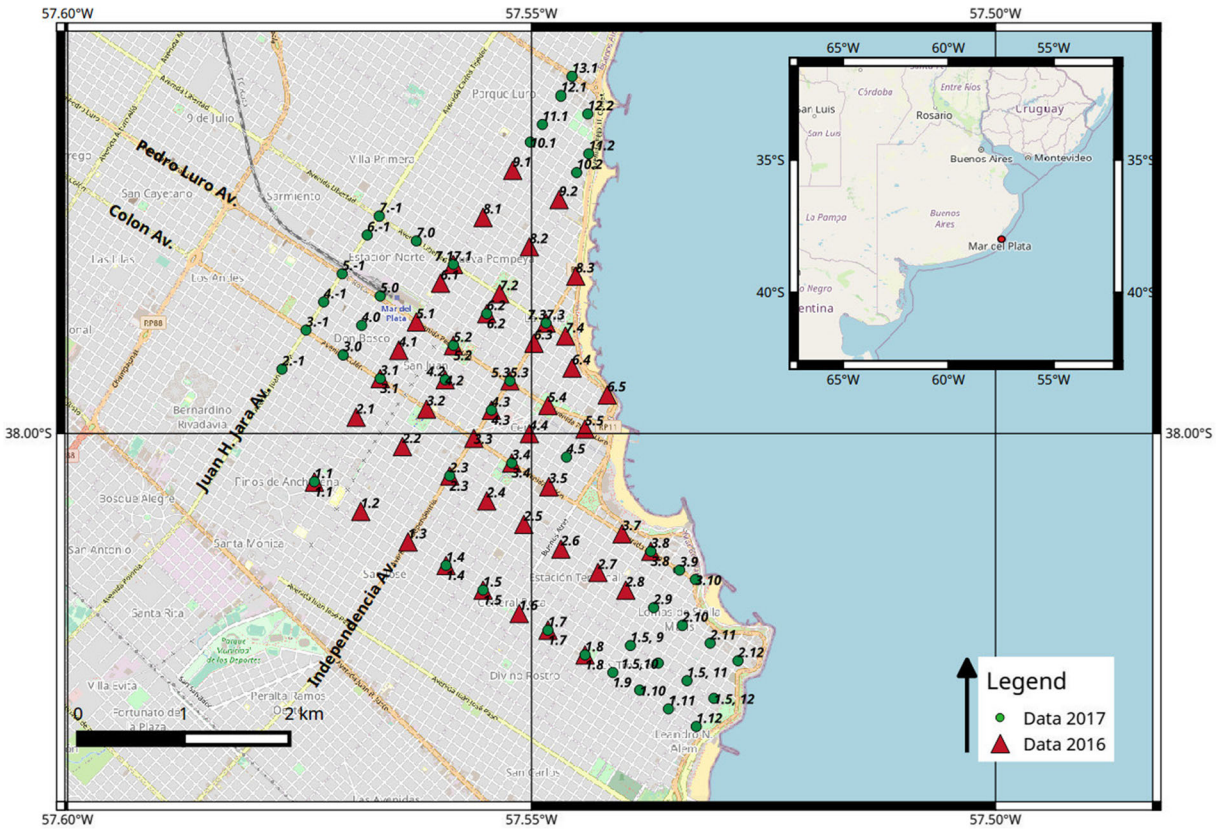

Fig. 1 Mar del Plata City (Argentina) and the sampling area for lichen collection in 2016 and 2017

collected by lichens, as well as their elemental composition.

The relationship between magnetic parameters and PTE was studied by a principal component analysis (PCA) with matrix correlation. Geostatistical methods were used for the estimation and spatial prediction of χ data. Firstly, a geostatistical model was built through a semi-variogram in order to describe the spatial relationship between the observed (measured) data points. If $Z(x_\alpha)$ are the observed data points, then the estimation of some data point in the space at position x_0 is made by (1):

$$Z^*(x_0) = \sum_{\alpha=1}^{n} \lambda_\alpha Z(x_\alpha) \quad (1)$$

where weights λ_α are estimated using the semi-variogram, which is a distinctive advantage in relation to other linear interpolation estimators. Moreover, its construction makes it as an optimum predictor of minimum variance. In practice, a number of sampling points are defined in the study area for making predictions at everywhere within this area. Secondly, the Ordinary Kriging Method (OKM) was used to build prediction maps of the magnetic proxy χ for both campaigns 2016 and 2017. Statistical analyses were performed using the R free software: R version 3.5.2 (R Core Team 2018).

3 Results and Discussion

3.1 Magnetic Particles on Lichen's Thallus

Magnetic enhancement on lichen's thallus is based on two contrasting magnetic materials: ferro-/ferrimagnetic and diamagnetic materials. Ferrimagnetic (magnetite) and ferromagnetic (iron) materials (with specific magnetic susceptibility $\chi = 0.4 - 1.1 \times 10^{-3}$ m^3 kg^{-1}, and $\chi = 2.8 \times 10^{-3}$ m^3 kg^{-1}, respectively) are much different from the diamagnetic matrix of organic thallus ($\chi = -0.9 \times 10^{-8}$ m^3 kg^{-1}; Maher and Thompson 1999). Magnetic parameters and related ratios were determined for all lichen samples and descriptive statistics of them are detailed in Table 1.

Ferrimagnetic minerals are dominant (over antiferromagnetic ones) magnetic particles present in lichen's thallus as indicated by results of S-ratio. Values of this ratio are about 0.90 (ml samples) and 0.92 (mlv samples) for both campaigns (Fig. 2a).

Among these dominant ferrimagnetic minerals, magnetite is the main magnetic carrier determined from an integrated analysis of thermomagnetic curves, acquisition IRM curves, and parameter H_{cr}, which varied between 33.9–40.5 mT for 2016 and 33.1–40.6 mT for 2017 (Fig. 2a). These ranges fall within the reported values for magnetite (8.0–69.5 mT, Peters and Dekkers 2003). Although H_{cr} may vary with grain size of magnetic minerals, a mixture of low- and high-coercivity minerals may also lead to slight variations in H_{cr} as reported by Chaparro and Sinito (2004), Chaparro et al. (2020a), and references therein. Mean (and SD) values are similar for both campaigns and are interpreted in term of a common PM production source: traffic pollution. Thermomagnetic studies (M-T curves) confirm the presence of these low-coercivity magnetic phases (Fig. 2b). Curie temperatures (T_c) of different phases were determined in heating curves; they show the predominance of a main phase corresponding to magnetite (T_c = 550–577 °C) and also an additional minor phase of high-coercivity minerals that corresponds to hematite (T_c = 653–683 °C).

Samples with different vehicular influence and concentration of magnetic particles (e.g., χ = 159.0 and 54.3 × 10^{-8} m^3 kg^{-1} for ml-4.3 and mlv-7.0, respectively) were analyzed by SEM-EDS. SEM images of typical particles on lichen's thallus can be appreciated in Fig. 3; in addition, the morphological and compositional analysis by EDS is detailed in Table S1 and S2 (Supplementary Material).

The analysis of several particles reveals the presence of iron-rich particles with different morphologies and sizes, with a minimum of 0.5 μm, a maximum of 3 μm, and a mean (± SD) of 1.5 ± 0.8 μm in size (Table S1, Supplementary Material). In particular, size of iron-rich semi-spherules is 1.3 ± 0.7 μm, and the size of irregular iron-rich particles is 1.8 ± 0.8 μm. Such values are consistent with particle sizes found through the analysis of anhysteretic ratios χ_{ARM}/χ and ARM/SIRM (Table 1), being all breathable sizes ($PM_{2.5}$).

The EDS analysis allows us to identify and quantify iron-rich particles (Fe contents of 30–97 wt%, Table S2, Supplementary Material); it also allows to find elements such as Na, Mg, Al, Si, S, Cl, K, Ca, Ti, Cr, Mn, Ni, and Ag and determine their concentrations, which are consistent with the chemical analysis carried out by ICP-OES. Most of PTE are associated with the observed iron-rich particles.

Iron-oxide spherules and irregular particles are common components of the $PM_{2.5}$, PM_{10}, and PTE emitted by exhaust pipes from gasoline and diesel engines (exhaust emissions), wear from brake linings, and tires by vehicles, as reported by Sagnotti et al. (2009) and Chaparro et al. (2010).

Grain-size distribution of the main magnetic carrier, i.e., magnetite, is determined from anhysteretic ratios χ_{ARM}/χ, ARM/SIRM, and reference values for magnetite (King et al. 1982) that are presented in Fig. 4. Although hematite is also detected by thermomagnetic studies, its content is not dominant (S-ratio ≈ 0.90–0.92) enough to have influence on the particle size inference of magnetite. According to Frank and Nowacyk (2008), variations in hematite content can be ignored when interpreting grain size indicative parameters for samples where hematite contents range from 0 to 98 wt%. Most of analyzed samples (ml and mlv) show magnetic particles ≤ 1 μm in size, which are categorized as $PM_{2.5}$, inhalable particle sizes as concluded by SEM-EDS analysis (Fig. 3) as well. They are extremely dangerous particles for human health because of their capacity for traveling long distances and reaching deep into the lungs, as well as other human organs (Calderón-Garcidueñas et al. 2019).

3.2 Potentially Toxic Elements and Magnetic Proxies for Air Particle Pollution

From the element determinations by ICP-OES for 30 lichen samples, the presence of PTE (such as Ba, Cu, Cr, Co, Fe, Mo, Ni, Pb, V, and Zn) was determined; some of which were detected by EDS as well. These elements constitute a potential health risk and some of them have high mean (± SD) concentration values, i.e., Ba (77.2 ± 29.1 mg/kg), Co (2.0 ± 1.2 mg/kg), Cr (7.4 ± 3.4 mg/kg), Cu (38.6 ± 13.0 mg/kg), Mo (1.3 ± 0.5 mg/kg), Ni (3.3 ± 1.1 mg/kg), Pb (32.3 ± 20.2 mg/kg), V (7.4 ± 2.7 mg/kg), Zn (1.3 ± 0.5 g/kg), and Fe (5.1 ± 2.0 g/kg). The corresponding descriptive statistics are shown in Figure S1 (Supplementary Material). Most of these PTE are statistically correlated between them. The highest R-values are, in particular, between Ba, Cr, Ni, and V with Fe ($R = 0.70 - 0.95$, $p < 0.01$; Table S3, Supplementary Material), which is explained by

Table 1 Descriptive statistics for magnetic parameters of ml and mlv samples, Campaign 2016 and 2017, respectively

	Campaign 2016 (N= 53)				*Campaign 2017 (N= 52)*			
	Mean	SD	Min.	Max.	Mean	SD	Min.	Max.
χ [10^{-8} m^3kg^{-1}]	119.3	38.4	60.6	218.6	75.6	48.5	12.4	210.1
ARM [10^{-6} Am^2kg^{-1}]	392.0	108.4	197.9	628.7	211.2	121.0	32.7	521.8
SIRM [10^{-3} Am^2kg^{-1}]	13.4	4.1	7.6	22.0	8.0	5.1	1.6	20.5
χ_{ARM} [10^{-8} m^3kg^{-1}]	554.5	222.5	232.8	1643.7	260.5	151.0	42.6	616.1
χ_{fd}% [%]	3.6	2.0	0.5	10.7	2.6	2.2	0.0	9.8
ARM/SIRM [a.u.]	0.03	0.01	0.01	0.04	0.03	0.00	0.02	0.04
χ_{ARM}/χ [a.u.]	5.0	2.3	1.7	15.5	3.7	0.8	2.2	6.1
SIRM/χ [kA/m]	11.8	1.8	7.7	17.6	10.8	1.3	8.3	14.2
H_{cr} [mT]	38.2	1.3	40.5	33.9	37.0	1.8	33.1	40.6
S-ratio [a.u.]	--	--	0.58	1	--	--	0.78	1

S-ratio data are constrained to a 1-D unit simplex; hence, both mean and standard deviation were not calculated

compounds that come from exhaust and brake emissions reported by Maher et al. (2008) and Chaparro et al. (2010). It can be observed that these emitted PTE coincide with most of elements reported previously.

Initially, the correlation matrix was generated with all variables, that is 10 magnetic and 10 chemical variables, and the Kaiser-Meyer-Olkin (KMO, Pérez 2004) test was applied, testing with different variables until a good index value was obtained (KMO = 0.55 for 16 selected variables). Thus, the PCA with correlation matrix was performed using a total of 16 variables, i.e., 10 chemical (Ba, Co, Cr, Cu, Fe, Mo, Ni, Pb, V, and Zn) and 6 magnetic (χ, ARM, SIRM, ARM/SIRM, SIRM/χ, and H_{cr}) variables, which include concentration, mineralogy, and grain size variables. The three principal components (PC) explained 77.7% of the observed variance. This high value represents a good reduction of dimensions and the high quality of the dataset representation. Correlations of variables with each PC are detailed in Table 2. PC1 is defined by magnetic concentration and chemical variables that show positive correlation (0.46–0.97) in the following order: Cr > Ni > Fe > V > Cu > Zn > Ba > χ > ARM > Mo > SIRM. The second component, PC2, is only constituted by ARM/SIRM, which is related to the magnetic grain size; and PC3 is only associated with the magnetic mineralogical parameter H_{cr}.

Taken into account the composition of PM pollutants emitted by vehicular traffic, it is easily explained why most of all PTE and concentration-dependent magnetic parameters are grouped in the same PC (PC1).

Although relevant properties, such as concentration and size, of trapped magnetic particles are fundamental for magnetic biomonitoring, the correlation between concentration-dependent magnetic parameters and most of all PTE proved a common origin of both pollutants. It allows us to identify relevant magnetic parameters and therefore to determine magnetic proxies for air particle pollution. These magnetic parameters (χ, ARM, and SIRM) associated with PTE are potential magnetic proxies for biomonitoring studies in this urban area and others where traffic emission is one of the main pollution sources. However, magnetic susceptibility is perhaps the best proxy for pollution that has been used in many studies. χ has the advantage to be determined with high sensitivity combined with fast laboratory processing; sample preparation is easy, laboratory instruments are of relatively low cost, and most measurements are nondestructive (Chaparro et al. 2020b). In this case of study, correlations for PC1 (Table 2) allow us to propose χ as a magnetic proxy for Cr, Ni, Fe, V, Cu, Zn, Ba, and Mo pollution. As mentioned, these PTE come from exhaust, general corrosion, and brake emissions as reported by Lu et al. (2005), Maher et al. (2008), Sagnotti et al. (2009), and Chaparro et al. (2010), among others.

3.3 Spatial Distribution of Particle Pollution

Geostatistical analysis for biomonitoring based on magnetic susceptibility has been performed in different polluted environments. Among them, results

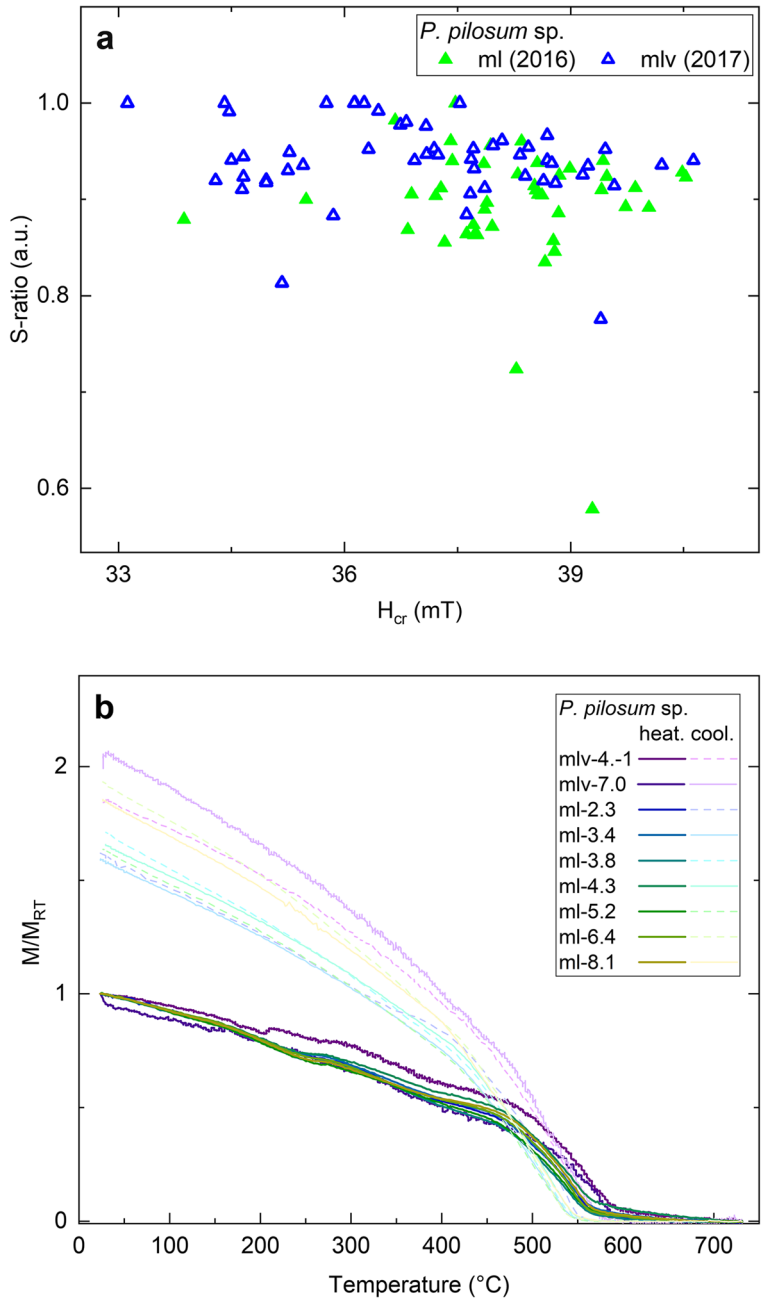

Fig. 2 (**a**) Biplot S-ratio and H_{cr} and (**b**) thermomagnetic measurements (heating and cooling runs) for lichen samples ml (2016) and mlv (2017)

obtained in a high-precipitation tropical valley proved the potential of combined analyses for determining the highest magnetic PM concentration within a large area of 290 km^2, that is, adversely impacted zones where most human activities were concentrated (Mejía-Echeverry et al. 2018). As mentioned, χ is one of the most widely used magnetic proxies for air particle pollution.

Different empirical semi-variograms of χ were constructed in order to get the best spatial correlation model. The best fitting was obtained using a theoretical exponential model as shown in Figure S2 (Supplementary Material). A maximum distance of 0.015 degrees (≈ 1500 m) and 5 adjustment points were selected; hence, the fitting of the empirical semivariogram was made by the method of heavy least

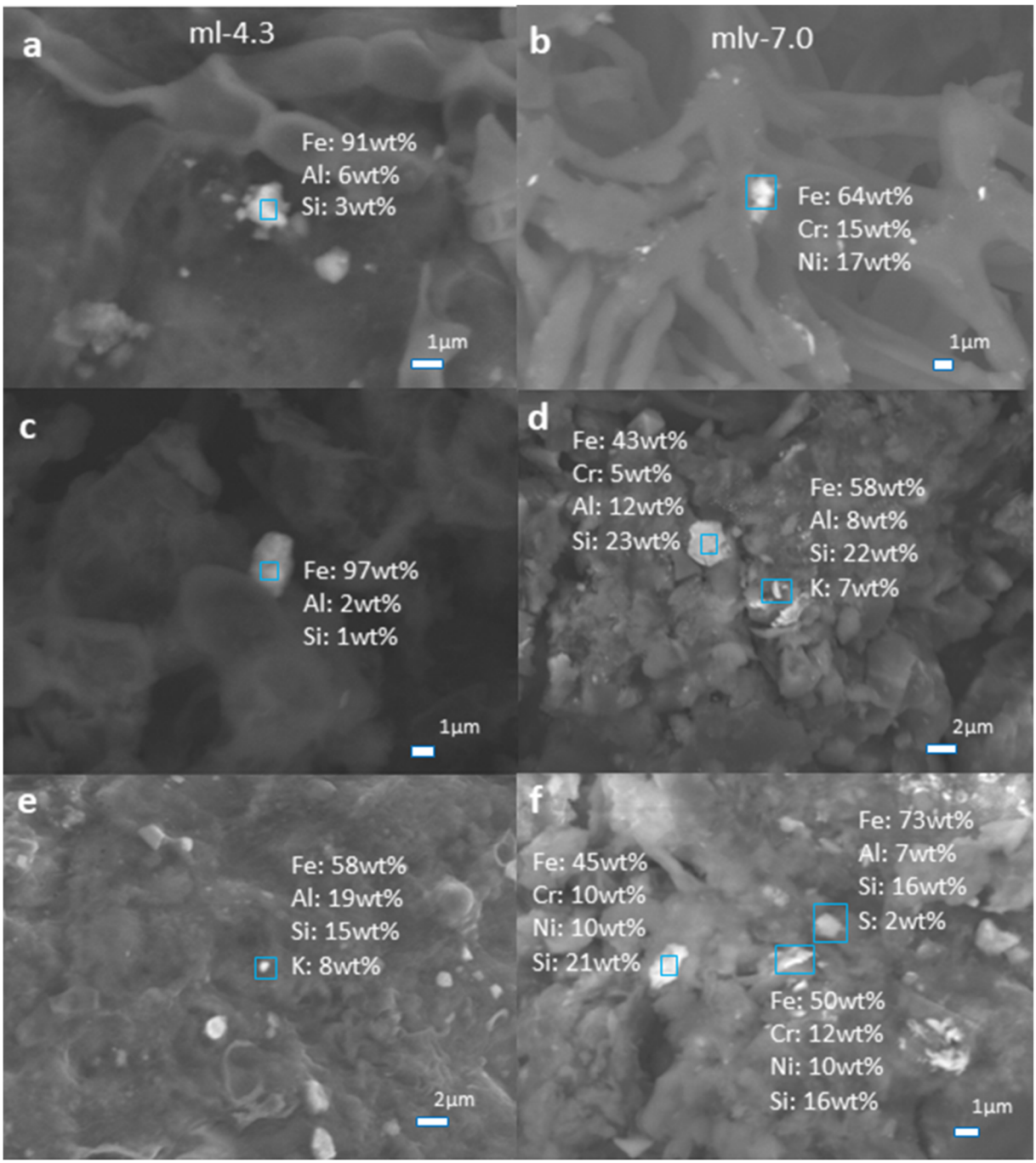

Fig. 3 SEM-EDS analysis. Observations made on different parts of the lichen's thallus corresponding to samples ml-4.3 (a, c, e) and mlv-7.0 (b, d, e)

squares. The OKM was used for χ-data from both sampling campaign, for which a grid of 0.0001 degrees was used, and therefore, about 295,000 points for the Campaign 2016, and 310,000 points for the Campaign 2017 were considered. It is worth mentioning that the predicted values depend on neighboring observed data points where spatial continuity is assumed, but they do not depend on the number of points. Two prediction maps were generated for χ and represented in Fig. 5.

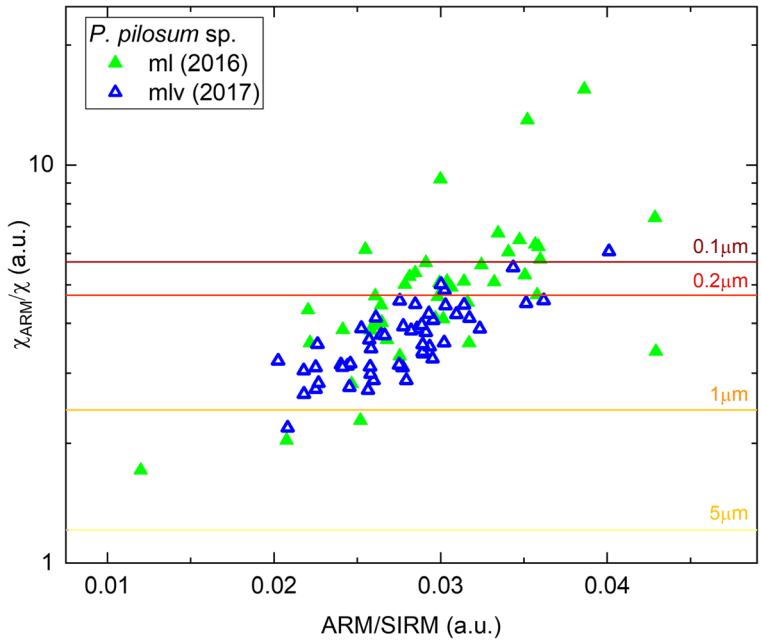

Fig. 4 Biplot of anhysteretic ratios χ_{ARM}/χ and ARM/SIRM for samples collected in 2016 and 2017. Reference lines of magnetic particle size are based on King et al. (1982)

As observed, the highest concentration areas in 2016 ($\chi > 130 \times 10^{-8}$ m^3kg^{-1}) are located in downtown Mar del Plata, involving roads with high traffic emissions such as Luro Ave., Colon Ave. and Independencia Ave. Comparison of these maps shows that areas of low magnetic concentration are relatively similar between 2016 (Fig. 5a) and 2017 (Fig. 5b), but not for those areas of the highest χ values. For example, downtown is not a hotspot in 2017, decreasing its χ value from 130 to 80 × 10^{-8} m^3kg^{-1}. In this last campaign, high concentration areas move towards areas limited by Jara Ave. between Luro Ave. and Colon Ave., and Independencia Ave. and Alberti St., which become critical areas with χ values of 160×10^{-8} m^3kg^{-1} and 120×10^{-8} m^3kg^{-1}, respectively. In general, a decrease in magnetic concentration (χ) in 2017 is observed, which may be explained through the rainfall influence during the period of this study.

Table 2 Correlations of each variable with each PC, results obtained from PCA

Variable	PC1	PC2	PC3	% Total reconstruction
χ	**0.60**	0.04	0.23	**0.87**
ARM	**0.57**	0.02	0.24	**0.83**
SIRM	**0.46**	0.19	0.28	**0.93**
ARM/SIRM	0.00	**0.83**	0.00	**0.83**
SIRM/χ	0.14	0.17	0.01	0.32
H_{cr}	0.12	0.03	**0.55**	**0.70**
Ba	**0.64**	0.01	0.18	**0.83**
Co	0.32	0.27	0.00	**0.59**
Cr	**0.97**	0.00	0.00	**0.97**
Cu	**0.74**	0.06	0.08	**0.88**
Fe	**0.89**	0.09	0.00	**0.98**
Mo	**0.53**	0.06	0.02	**0.61**
Ni	**0.95**	0.00	0.02	**0.97**
Pb	0.37	0.01	0.03	0.41
V	**0.78**	0.13	0.00	**0.91**
Zn	**0.64**	0.14	0.03	**0.81**

3.4 Comparison Between Campaigns and with Other Related Studies

Magnetic measurements performed on samples ml and mlv show concentration-dependent magnetic parameter with similar ranges for 2016 ($\chi = 60.6$–218.6×10^{-8} m^3kg^{-1}, SIRM = 7.6–22.0 × 10^{-3} Am^2kg^{-1}) to 2017 ($\chi = 12.4$–210.1×10^{-8} m^3kg^{-1}, SIRM = 1.6–20.5 × 10^{-3} Am^2kg^{-1}), where the highest concentrations of magnetic particles correspond to sampling sites with high vehicular influence or traffic. Although samples ml and mlv have similar ranges of mentioned concentration parameters, mean values of samples decrease about 40% from 2016 to 2017.

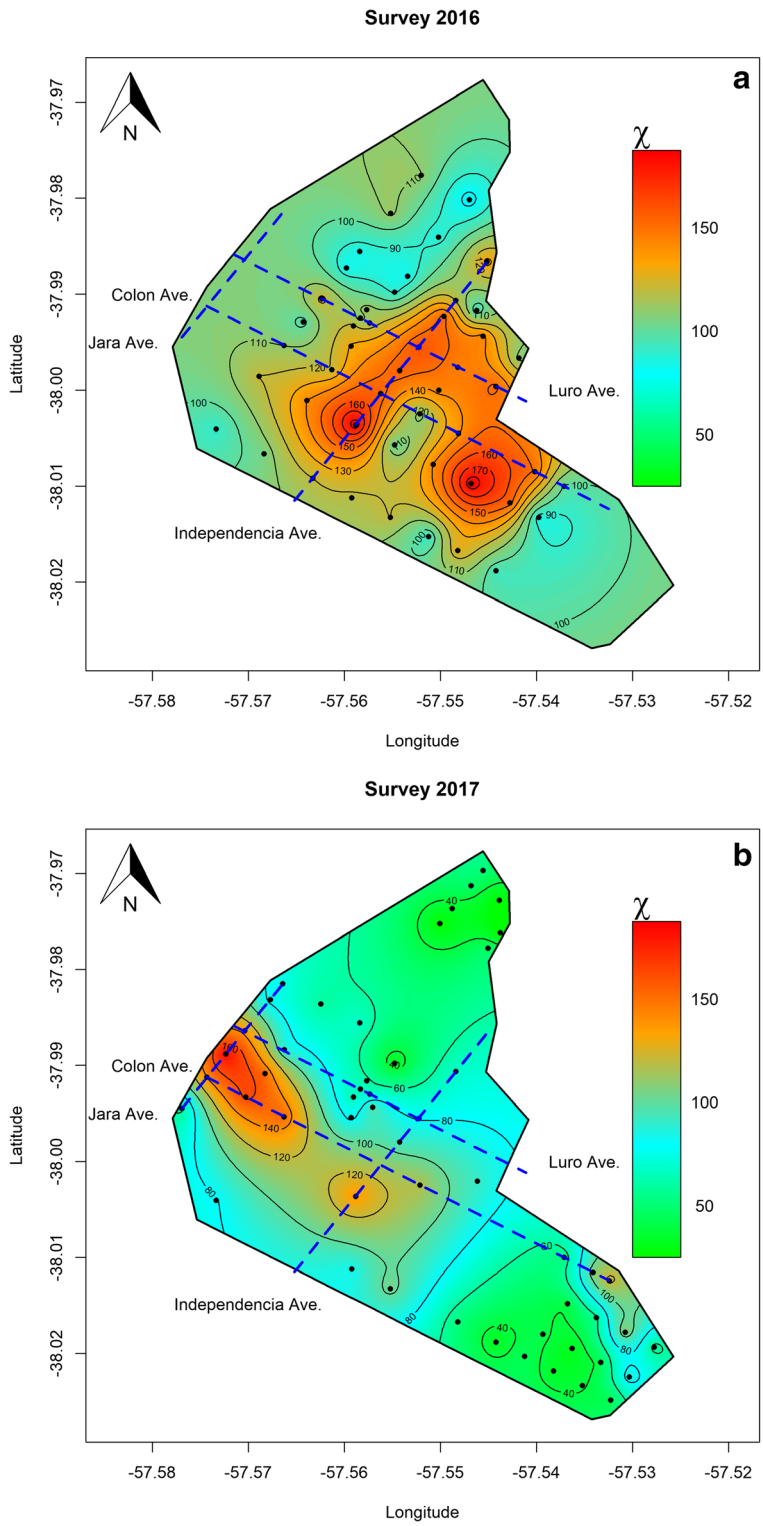

Fig. 5 Prediction maps by the Ordinary Kriging Method based on χ (in 10^{-8} m^3kg^{-1}) for both campaigns (a) 2016 and (b) 2017

This general decrease in the magnetic concentration for 2017 may be explained through the influence of meteorological conditions. In particular, several days of intense rain took place before the campaign 2017

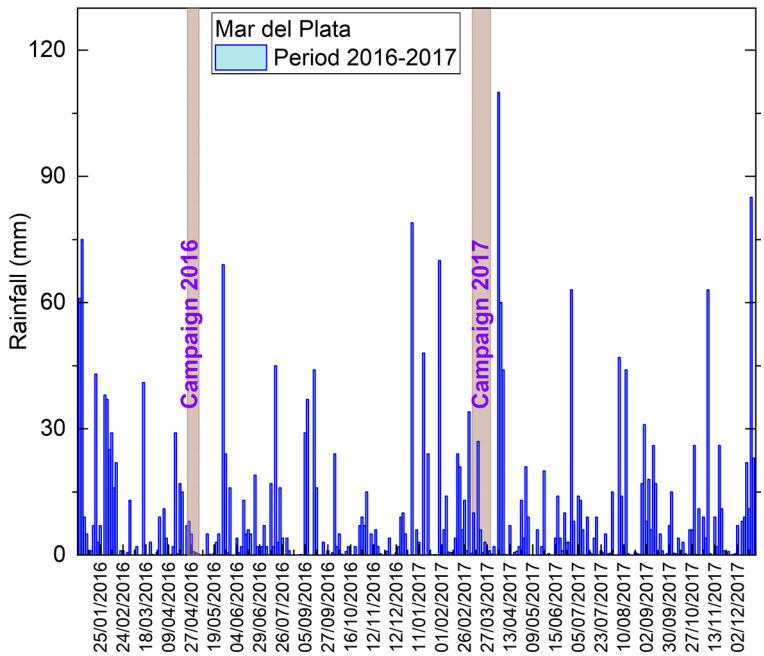

Fig. 6 Rainfall data for Mar del Plata City recorded by the National Meteorological Service from January 2016 to December 2017 (CIM 2020). Collection of lichens of both campaigns, i.e., Campaign 2016 (25 April 2016–05 May 2016) and Campaign 2017 (06 March 2017–29 March 2017), is indicated

(CIM 2020) as observed in Fig. 6. Mar del Plata has a high annual precipitation (up to 900 mm) and seasons are humid and moderate.

Rainfall seems to affect the concentration of PM trapped by lichens. Marié et al. (2018) reported the influence of rain precipitation on the magnetic signal measured in lichen's thallus (of *P. pilosum*). In their annual records, with weekly measurements of in situ magnetic susceptibility κ_{is}, they observed changes (decreases) in the mean values of κ_{is} after moderate to intense periods of rain. Such changes are related to a partial washing of the particles trapped on the lichen's thallus, as well as a reduction of PM in the air by wet deposition. Such decrease, and hence partial loss of magnetic particles, may be explained by results concluded for transplanted *P. pilosum* as well.

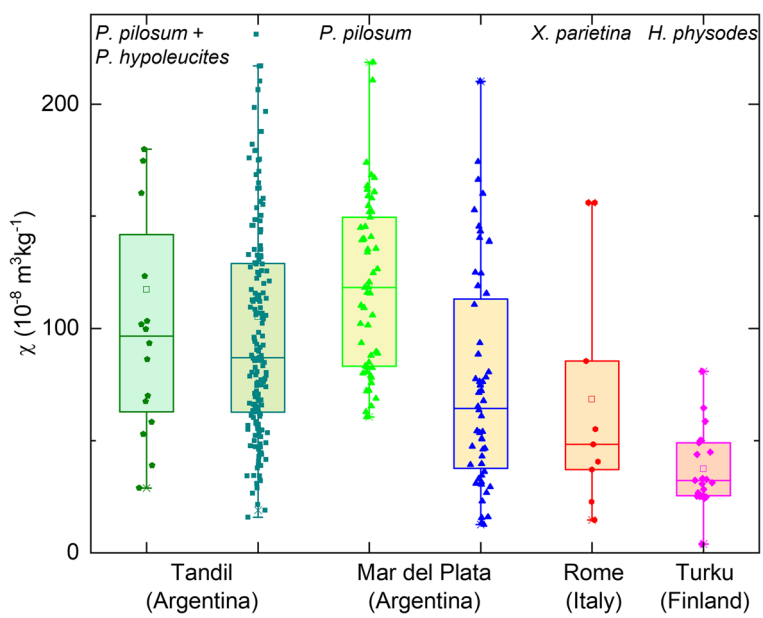

Fig. 7 Comparison of magnetic biomonitoring studies using native lichens in Mar del Plata (Campaigns 2016 and 2017, this study), Tandil (Chaparro et al. 2013; Marié et al. 2016), Rome (Winkler et al. 2019), and Turku (Salo et al. 2012). Box delineates interquartile range 25–75% (Q1–Q3) and the horizontal line in box indicates the median. Mean value is indicated with an open square; minimum and maximum values are shown using whiskers

Recently, Marié et al. (2020) found decreases of 5–28% in χ after rainy month periods.

Among these parameters, χ is dependent on the concentration of all magnetic particles accumulated in each sample. On the other hand, SIRM only depends on the concentration of ferrimagnetic particles. Both parameters are significantly correlated ($R = 0.95$, $p < 0.01$) indicating the dominance of the ferrimagnetic carrier magnetite (Sect. 3.1). Differences in magnetic susceptibility between both campaigns can be observed in Fig. 7, the quartile values (Q1–Q3) are higher for 2016 ($\chi = 83.1 - 149.5 \times 10^{-8}$ m^3kg^{-1}) than for 2017 ($\chi = 37.6 - 113.1 \times 10^{-8}$ m^3kg^{-1}), and mean values are up to twofold higher in 2016 ($\chi = 119.3 \times 10^{-8}$ m^3kg^{-1}) than in 2017 ($\chi = 75.6 \times 10^{-8}$ m^3kg^{-1}). This fact indicates that there is not only difference in concentrations of magnetic minerals between sites, but also between periods of time, i.e., different levels of accumulation of magnetic particles related to airborne particle contamination.

Results obtained for this study are compared with other magnetic biomonitoring using native (or in situ) lichen as well. Magnetic concentration values reported by Chaparro et al. (2013) and Marié et al. (2016) in Tandil (Argentina) are similar to χ values from Mar del Plata. As appreciated in Fig. 7, mean (± SD) values of χ are 117.3 ± 96.8 and $105.1 \pm 94.1 \times 10^{-8}$ m^3kg^{-1} for Tandil, being slightly lower than values of ml data (2016) and higher than of mlv data (2017). Although both cities have different population, Mar del Plata has about 619,000 inhabitants and Tandil has about 120,000; the last city seems to be comparable in magnetic concentration values because of, in addition to traffic emissions, the contribution of PM from metallurgical factories within the urban area. It is worth mentioning that this comparison in both Argentinian cities involves the same species *Parmotrema pilosum* and *Punctelia hypoleucites*.

On the other hand, comparison with studies carried out far away from the study area evidences lower mean (± SD) values of $\chi = 68.4 \pm 53.6 \times 10^{-8}$ m^3kg^{-1} for Rome (Italy, Winkler et al. 2019) and $\chi = 37.4 \pm 17.1 \times 10^{-8}$ m^3kg^{-1} for Turku (Finland, Salo et al. 2012). Among possible causes of such differences, (a) other native species (*Xanthoria parietina* and *Hypogymnia physodes*) were used in those European cities. In addition to the number of studied samples between studies, (b) latitude and climatic condition seems to be the most remarkable difference for native species' collection of magnetic PM. For example, Turku is a city (of about 180,000 inhabitants) located at high/mid latitude (60° N) where summer and winter seasons are well distinctive from this study. This distinctive difference between seasons at high-latitude areas may reduce the exposure time of native lichen's thallus throughout the year and its lifetime; in particular, snow cover hinders particle accumulation of in situ species (Salo 2016). On the other hand, Rome (a city of about 2.9 million inhabitants) data shows χ values similar to this study, which may be due to its latitude (41° N) comparable to Mar del Plata (38° S). Other possible causes can be related to (c) the collection methodology for each study, as well as (d) the sampling season: collection for this study was carried out in autumn, for Tandil was done throughout the year, for Turku is not specified, and in Rome was done in summer. Autumn and winter seasons are recommended for biomonitoring because in this leafless time the disturbing effect of vegetation (trapping pollutants) is minimal (Salo 2016). Furthermore, Marié et al. (2018) reported an inverse relation between magnetic susceptibility and temperature for 1 year of measurements, i.e., a trend of increasing κ_{is} values during seasons of lower temperatures.

4 Conclusion

Magnetic biomonitoring using native lichens is a complementary method to those that already exist, with the advantage of low cost, both in time and money, and which allows for evaluating the air particle pollution in cities with available species in a simple manner.

Magnetic PM collected by lichen's thallus is identified as magnetite-like minerals of ≤ 1 μm in size with morphologies of spherules and irregular particles. Such Fe-rich particles by vehicle emissions are associated with potentially toxic elements as determined by EDS and ICP. This is also concluded by PCA through the first PC defined by variables χ, ARM, SIRM, Cr, Ni, Fe, V, Cu, Zn, Ba, and Mo. Both, size and composition, are extremely dangerous particles for human health and living beings. Correlations between concentration-dependent magnetic parameters and PTE allow us to propose χ as a magnetic proxy for Cr, Ni, Fe, V, Cu, Zn, Ba, and Mo pollution in this urban area and similar ones.

Comparison with other related studies shows similar magnetic susceptibility ranges with another city from

Argentina where native species *P. pilosum* and *P. hypoleucites* were used. The reported values for European cities are lower than the present study; such differences may be due to, among others factors, the use of other native species (*X. parietina* and *H. physodes*), latitude location (41° N and 60° N), climatic conditions, collection methodology, and sampling season. Prediction maps of χ are valuable piece of information for the study area showing the most impacted zones, which are located on main access and avenues with important vehicle traffic. These maps also show changes over time, i.e., concentrations of magnetic particles decrease from 2016 to 2017. Rainfall seems to affect particle collection, leading to a partial loss of particles from lichen's thallus. Therefore, special care should be taken for collection of lichen after rainy periods.

Supplementary Information The online version contains supplementary material available at https://doi.org/10.1007/s11270-021-05047-w.

Acknowledgments The authors wish to thank the Universidad Nacional del Centro de la Provincia de Buenos Aires (UNCPBA), the Universidad Nacional Autónoma de México (UNAM), and the National Council for Scientific and Technological Research (CONICET) for their financial support. This contribution was supported by Agencia Nacional de Promoción Científica y Tecnológica Project PICT-2013-1274, the Bilateral CONICET/CONACYT Project No. 207149 (Harald Böhnel) and Res. 1001/14 - 5131/15 (Marcos Chaparro), and the Scholarship EVC-CIN-2018 (Rocío Gómez). The authors thank the anonymous reviewers whose comments improved the manuscript. They also thank Dr. M. Vega González (CGEO-UNAM), Ing. J. Escalante (CGEO-UNAM), and Michael Paarlberg for their technical support.

Declarations

Conflict of Interest The authors declare no conflict of interest.

References

Almeida, S. M., Pio, C. A., Freitas, M. C., Reis, M. A., & Trancoso, M. A. (2005). Source apportionment of fine and coarse particulate matter in a sub-urban area at the Western European Coast. *Atmospheric Environment, 39*, 3127–3138. https://doi.org/10.1016/j.atmosenv.2005.01.048.

Bermudez, G. M. A., Rodriguez, J. H., & Pignata, M. L. (2009). Comparison of the air pollution biomonitoring ability of three *Tillandsia* species and the lichen *Ramalina celastri* in Argentina. *Environmental Research, 109*, 6–14. https://doi.org/10.1016/j.envres.2008.08.014.

Block, M. L., & Calderón-Garcidueñas, L. (2009). Air pollution: Mechanisms of neuroinflammation and CNS disease. *Trends in Neurosciences, 32*(9), 506–516. https://doi.org/10.1016/j.tins.2009.05.009.

Boamponsem, L. K., & de Freitas, C. R. (2017). Validation of *Parmotrema reticulatum* as a biomonitor of elemental air pollutants in Auckland, New Zealand. *Journal of the Royal Society of New Zealand 47*(4), 275–293. https://doi.org/10.1080/03036758.2017.1296472

Brauer, M., Hoek, G., Van Vliet, P., Meliefste, K., Fischer, P. H., Wijga, A., et al. (2002). Air pollution from traffic and the development of respiratory infections and asthmatic and allergic symptoms in children. *American Journal of Respiratory and Critical Care Medicine, 166*(8), 1092–1098. https://doi.org/10.1164/rccm.200108-007OC.

Calderón-Garcidueñas, L., González-Maciel, A., Mukherjee, P. S., Reynoso-Robles, R., Pérez-Guillé, B., Gayosso-Chávez, C., Torres-Jardón, R., Cross, J. V., Ahmed, I. A. M., Karloukovski, V. V., & Maher, B. A. (2019). Combustion- and friction-derived magnetic air pollution nanoparticles in human hearts. *Environmental Research, 176*, 108567. https://doi.org/10.1016/j.envres.2019.108567.

Calvelo, S., & Liberatore, S. (2004). Applicability of in situ or transplanted lichens for assessment of atmospheric pollution in Patagonia, Argentina. *Journal of Atmospheric Chemistry, 49*, 199–210. https://doi.org/10.1007/s10874-004-1225-8.

Carreras, H. A., & Pignata, M. L. (2002). Biomonitoring of heavy metals and air quality in Córdoba City, Argentina, using transplanted lichens. *Environmental Pollution, 177*, 77–87. https://doi.org/10.1016/s0269-7491(01)00164-6.

Castañeda-Miranda, A. G., Chaparro, M. A. E., Chaparro, M. A. E., & Böhnel, H. N. (2016). Magnetic properties of *Tillandsia recurvata* L. and its use for biomonitoring a Mexican metropolitan area. *Ecological Indicators, 60*, 125–136. https://doi.org/10.1016/j.ecolind.2015.06.025.

Chaparro, M. A. E., & Sinito, A. M. (2004). An alternative experimental method to discriminate magnetic phases using IRM acquisition curves and magnetic demagnetisation by alternating field. *Revista Brasileira de Geofísica, 22*(1), 17–32. https://doi.org/10.1590/S0102-261X2004000100002.

Chaparro, M. A. E., Marié, D. C., Gogorza, C. S. G., Navas, A., & Sinito, A. M. (2010). Magnetic studies and scanning electron microscopy X-ray energy dispersive spectroscopy analyses of road sediments, soils, and vehicle-derived emissions. *Studia Geophysica et Geodaetica, 54*, 633–650. https://doi.org/10.1007/s11200-010-0038-2.

Chaparro, M. A. E., Lavornia, J. M., Chaparro, M. A. E., & Sinito, A. M. (2013). Biomonitors of urban air pollution: Magnetic studies and SEM observations corticolous foliose and microfoliose lichens and their suitability for magnetic monitoring. *Environmental Pollution, 172*, 61–69. https://doi.org/10.1016/j.envpol.2012.08.006.

Chaparro, M. A. E., Gargiulo, J. D., Irurzun, M. A., Chaparro, M. A. E., Lecomte, K. L., Böhnel, H. N., Córdoba, F. E., Vignoni, P. A., Manograsso-Czalbowski, N. T., Lirio, J. M., Nowaczyk, N. R., & Sinito, A. M. (2014). Magnetic parameters in paleolimnological studies in Antarctica ["El uso de parámetros magnéticos en estudios

paleolimnológicos en Antártida"]. *Latin American Journal of the Sedimentology and Basin Analysis, 21*, 77–96 http://ppct.caicyt.gov.ar/index.php/lajsba/article/view/5426/6276.

Chaparro, M. A. E., Moralejo, M. P., Böhnel, H. N., & Acebal, S. G. (2020a). Iron oxide mineralogy in Mollisols, Aridisols and Entisols from southwestern Pampean region (Argentina) by environmental magnetism approach. *Catena, 190*, 104534. https://doi.org/10.1016/j.catena.2020.104534.

Chaparro, M. A. E., Ramírez-Ramírez, M., Chaparro, M. A. E., Miranda-Avilés, R., Puy-Alquiza, M. J., Böhnel, H. N., & Zanor, G. A. (2020b). Magnetic parameters as proxies for anthropogenic pollution in water reservoir sediments from Mexico: An interdisciplinary approach. *Science of the Total Environment, 700*, 134343. https://doi.org/10.1016/j.scitotenv.2019.134343.

Centro de Información Meteorológica (CIM) (2020). *Data for period January 2016–December 2017 provided by the National Meteorological Service*. Website: https://www.smn.gob.ar/ Accessed 09 June 2020.

Escalante, J. E., & Böhnel, H. N. (2011). Diseño y Construcción de una Balanza de Curie [Design and construction of a Curie Balance]. *Geos, 31*(1), 63.

Evans, M., &Heller F. (2003). Environmental magnetism: Principles and applications of Enviromagnetics; Academic Press: Massachusetts, MA, USA, 299 pp.

Flanders, P. J. (1994). Collection, measurement, and analysis of airborne magnetic particulates from pollution in the environment. *Journal of Applied Physiology, 75*(10), 5931–5936. https://doi.org/10.1063/1.355518.

Frank, U., & Nowacyk, N. R. (2008). Mineral magnetic properties of artificial samples systematically mixed from haematite and magnetite. *Geophysical Journal International, 175*, 449–461. https://doi.org/10.1111/j.1365-246X.2008.03821.x.

Genc, S., Zadeoglulari, Z., Fuss, S. H., & Genc, K. (2012). The adverse effects of air pollution on the nervous system. *Journal of Toxicology, 2012*, 782462. https://doi.org/10.1155/2012/782462.

Huhn, G., Schulz, H., Stärk, H. J., Tölle, R., & Schüürmann, G. (1995). Evaluation of regional heavy metal deposition by multivariate analysis of element contents in pine tree barks. *Water, Air, and Soil Pollution, 84*, 367–383. https://doi.org/10.1007/BF00475349.

I Annual Report of Mar del Plata: Entre todos, monitoreo ciudadano (2015). http://www.mardelplataentretodos.org/documentos (4/01/2019, 16 hs).

Jordanova, D., Petrov, P., Hoffmann, V., Gocht, T., Panaiotu, C., Tsacheva, T., & Jordanova, N. (2010). Magnetic signature of different vegetation species in polluted environment. *Studia Geophysica et Geodaetica, 54*, 417–442. https://doi.org/10.1007/s11200-010-0025-7.

King, J., Banerjee, S. K., Marvin, J., & Özdemir, Ö. (1982). A comparison of different magnetic methods for determining the relative grain size of magnetite in natural materials: Some results from lake sediments. *Earth and Planetary Science Letters, 59*, 404–419. https://doi.org/10.1016/0012-821X(82)90142-X.

Kodnik, D., Winkler, A., Candotto Carniel, F., & Tretiach, M. (2017). Biomagnetic monitoring and element content of lichen transplants in a mixed land use area of NE Italy. *Science of the Total Environment, 595*, 858–867. https://doi.org/10.1016/j.scitotenv.2017.03.261.

Kováčik, J., Klejdus, B., Bačkor, M., Stork, F., & Hedbavny, J. (2011). Physiological responses of root-less epiphytic plants to acid rain. *Ecotoxicology, 20*, 348–357. https://doi.org/10.1007/s10646-010-0585-x.

Lawrence, S., Sokhi, R., Ravindra, K., Mao, H., Prain, H. D., & Bull, I. D. (2013). Source apportionment of traffic emissions of particulate matter using tunnel measurements. *Atmospheric Environment, 77*, 548–557. https://doi.org/10.1016/j.atmosenv.2013.03.040.

Lu, S.-G., Bai, S.-Q., Cai, J.-B., & Xu, C. (2005). Magnetic properties and heavy metal contents of automobile emission particulates. *Journal of Zhejiang University. Science, 6B*(8), 731–735. https://doi.org/10.1631/jzus.2005.B0731.

Maher, B. A., & Thompson, R. (1999). *Quaternary climates, environment and magnetism*. Cambridge: Cambridge University Press 390 pp.

Maher, B. A., Moore, C., & Matzka, J. (2008). Spatial variation in vehicle-derived metal pollution identified by magnetic and elemental analysis of road side tree leaves. *Atmospheric Environment, 42*, 364–373. https://doi.org/10.1016/j.atmosenv.2007.09.013.

Maher, B. A., Ahmed, I. A. M., Karloukovski, V., MacLaren, D. A., Foulds, P. G., Allsop, D., Mann, D. M. A., Torres-Jardón, R., & Calderon-Garcidueñas, L. (2016). Magnetite pollution nanoparticles in the human brain. *Proceedings of the National Academy of Sciences of the United States of America, 113*, 10797–10801. https://doi.org/10.1073/pnas.1605941113.

Marié, D. C., Chaparro, M. A. E., Irurzun, M. A., Lavornia, J. M., Marinelli, C., Cepeda, R., Böhnel, H. N., Castañeda, M. A. G., & Sinito, A. M. (2016). Magnetic mapping of air pollution in Tandil City (Argentina) using the lichen *Parmotrema pilosum* as biomonitor. *Atmospheric Pollution Research, 7*, 513–520. https://doi.org/10.1016/j.apr.2015.12.005.

Marié, D. C., Chaparro, M. A. E., Lavornia, J. M., Sinito, A. M., Castañeda-Miranda, A. G., Gargiulo, J. D., Chaparro, M. A. E., & Böhnel, H. N. (2018). Atmospheric pollution assessed by in situ measurement of magnetic susceptibility on lichens. *Ecological Indicators, 95*, 831–840. https://doi.org/10.1016/j.ecolind.2018.08.029.

Marié, D. C., Chaparro, M. A. E., Sinito, A. M., & Lavat, A. (2020). Magnetic biomonitoring of airborne particles using lichen transplants over controlled exposure periods. *SN Applied Science, 2*, 104. https://doi.org/10.1007/s42452-019-1905-2.

Mejía-Echeverry, D., Chaparro, M. A. E., Duque-Trujillo, J. F., Chaparro, M. A. E., & Castañeda-Miranda, A. G. (2018). Magnetic biomonitoring as a tool for assessment of air pollution patterns in a tropical valley using *Tillandsia* sp. *Atmosphere, 9*(7), 283. https://doi.org/10.3390/atmos9070000.

Mills, N. L., Donaldson, K., Hadoke, P. W., Boon, N. A., MacNee, W., Cassee, F. R., & Newby, D. E. (2009). Adverse cardiovascular effects of air pollution. *Nature Clinical Practice. Cardiovascular Medicine, 6*(1), 36–44. https://doi.org/10.1038/ncpcardio1399.

Nel, A. (2005). Air pollution-related illness: Effects of particles. *Science, 308*(5723), 804–806. https://doi.org/10.1126/science.1108752.

Pérez, C. (2004). *Técnicas de Análisis Multivariante de Datos*. Prentice Hall: Editorial Pearson 646 pp.

Peters, C., & Dekkers, M. (2003). Selected room temperature magnetic parameters as a function of mineralogy, concentration and grain size. *Physics and Chemistry of the Earth, 28*, 659–667. https://doi.org/10.1016/S1474-7065(03)00120-7.

R Core Team (2018). *R: a language and environment for statistical computing. R version 3.5.2. Vienna*: R Foundation for Statistical Computing. URL: http://www.R-project.org/

Rhoades, M.F., 1999. A review of lichen and bryophyte elemental content. Literature with Reference to Pacific Northwest Species, United States. Department of Agriculture, Mountlake Terrace. http://gis.nacse.org/lichenair/doc/PNW_LitReview.pdf

Rogge, W. F., Hildemann, L. M., Mazurek, M. A., Cass, G. R., & Simoneit, B. R. T. (1993). Sources of fine organic aerosol. 3. Road dust, tire debris, and organometallic brake lining dust: Roads as sources and sinks. *Environmental Science & Technology, 27*(9), 1892–1904. https://doi.org/10.1021/es00046a019.

Sagnotti, L., Taddeucci, J., Winkler, A., & Cavallo, A. (2009). Compositional, morphological, and hysteresis characterization of magnetic airborne particulate matter in Rome, Italy. *Geochemistry, Geophysics, Geosystems, 10*, Q08Z06. https://doi.org/10.1029/2009GC002563.

Salo, H. (2016). Application of magnetic biomonitoring in air pollution research: Spatio-temporal properties of magnetic particle matter. http://urn.fi/URN:ISBN:978-951-29-6668-4

Salo, H., Bucko, M. S., Vaahtovuo, E., Limo, J., Mäkinen, J., & Pesonen, L. J. (2012). Biomonitoring of air pollution in SW Finland by magnetic and chemical measurements of moss bags and lichens. *Journal of Geochemical Exploration, 115*, 69–81. https://doi.org/10.1016/j.gexplo.2012.02.009.

Sett, R., & Kundu, M. (2016). Epiphytic lichens: their usefulness as bioindicators of air pollution. *Donnish Journal of Research in Environmental Studies, 3*(3), 17–24.

Winkler, A., Caricchi, C., Guidotti, M., Owczarek, M., Macri, P., Nazzari, M., Amoroso, A., Di Giosa, A., & Listrani, S. (2019). Combined magnetic, chemical and morphoscopic analyses on lichens from a complex anthropic context in Rome, Italy. *Science of the Total Environment, 690*, 1355–1368. https://doi.org/10.1016/j.scitotenv.2019.06.526.

Zschau, T., Getty, S., Gries, C., Ameron, Y., Zambrano, A., & Nash, T. H. (2003). Historical and current atmospheric deposition to the epilithic lichen *Xanthoparmelia* in Maricopa County, Arizona. *Environmental Pollution, 125*(1), 21–30. https://doi.org/10.1016/S0269-7491(03)00088-5.

Terms and Conditions

Springer Nature journal content, brought to you courtesy of Springer Nature Customer Service Center GmbH (“Springer Nature”).
Springer Nature supports a reasonable amount of sharing of research papers by authors, subscribers and authorised users (“Users”), for small-scale personal, non-commercial use provided that all copyright, trade and service marks and other proprietary notices are maintained. By accessing, sharing, receiving or otherwise using the Springer Nature journal content you agree to these terms of use (“Terms”). For these purposes, Springer Nature considers academic use (by researchers and students) to be non-commercial.
These Terms are supplementary and will apply in addition to any applicable website terms and conditions, a relevant site licence or a personal subscription. These Terms will prevail over any conflict or ambiguity with regards to the relevant terms, a site licence or a personal subscription (to the extent of the conflict or ambiguity only). For Creative Commons-licensed articles, the terms of the Creative Commons license used will apply.
We collect and use personal data to provide access to the Springer Nature journal content. We may also use these personal data internally within ResearchGate and Springer Nature and as agreed share it, in an anonymised way, for purposes of tracking, analysis and reporting. We will not otherwise disclose your personal data outside the ResearchGate or the Springer Nature group of companies unless we have your permission as detailed in the Privacy Policy.
While Users may use the Springer Nature journal content for small scale, personal non-commercial use, it is important to note that Users may not:

1. use such content for the purpose of providing other users with access on a regular or large scale basis or as a means to circumvent access control;
2. use such content where to do so would be considered a criminal or statutory offence in any jurisdiction, or gives rise to civil liability, or is otherwise unlawful;
3. falsely or misleadingly imply or suggest endorsement, approval , sponsorship, or association unless explicitly agreed to by Springer Nature in writing;
4. use bots or other automated methods to access the content or redirect messages
5. override any security feature or exclusionary protocol; or
6. share the content in order to create substitute for Springer Nature products or services or a systematic database of Springer Nature journal content.

In line with the restriction against commercial use, Springer Nature does not permit the creation of a product or service that creates revenue, royalties, rent or income from our content or its inclusion as part of a paid for service or for other commercial gain. Springer Nature journal content cannot be used for inter-library loans and librarians may not upload Springer Nature journal content on a large scale into their, or any other, institutional repository.
These terms of use are reviewed regularly and may be amended at any time. Springer Nature is not obligated to publish any information or content on this website and may remove it or features or functionality at our sole discretion, at any time with or without notice. Springer Nature may revoke this licence to you at any time and remove access to any copies of the Springer Nature journal content which have been saved.
To the fullest extent permitted by law, Springer Nature makes no warranties, representations or guarantees to Users, either express or implied with respect to the Springer nature journal content and all parties disclaim and waive any implied warranties or warranties imposed by law, including merchantability or fitness for any particular purpose.
Please note that these rights do not automatically extend to content, data or other material published by Springer Nature that may be licensed from third parties.
If you would like to use or distribute our Springer Nature journal content to a wider audience or on a regular basis or in any other manner not expressly permitted by these Terms, please contact Springer Nature at

onlineservice@springernature.com